J|A|C|S
ARTICLES
Published on Web 04/11/2006

Lithiated Imines: Solvent-Dependent Aggregate Structures and Mechanisms of Alkylation

Stephan J. Zuend, Antonio Ramirez, Emil Lobkovsky, and David B. Collum*

Contribution from the Department of Chemistry and Chemical Biology, Baker Laboratory, Cornell University, Ithaca, New York 14853-1301

Received January 17, 2006; E-mail: dbc6@cornell.edu

Abstract: We describe efforts to understand the structure and reactivity of lithiated cyclohexanone *N*-cyclohexylimine. The lithioimine affords complex solvent-dependent distributions of monomers, dimers, and trimers in a number of ethereal solvents. Careful selection of solvent provides exclusively monosolvated dimers. Rate studies on the C-alkylations reveal chronic mixtures of monomer- and dimer-based pathways. We explore the factors influencing reactants and alkylation transition structures and the marked differences between lithioimines and isostructural lithium dialkylamides with the aid of density functional theory calculations.

Introduction

Many years ago we investigated the solid state and solution structures of lithiated *N*-phenylimine **1**. A combination of ^{6}Li and ^{15}N NMR spectroscopies revealed a mixture of monomers and dimers in THF. Competitive N- and C-alkylations of **1** posed a particularly interesting, but daunting, mechanistic problem.[1] Detailed studies of the N-alkylation in isolation using the isostructural lithium diphenylamide (**2**) uncovered an ensemble of mechanisms based on dimers, monomers, free ions, and mixed dimers.[2] Before investigating the C-alkylation in isolation using lithiated *N*-alkylimine **3** we became distracted by studies of synthetically important lithium amides exemplified by the isostructural lithium amide **4**[3]—studies that continued for almost two decades.[4] Although imines proved to be versatile substrates for investigating the reactivity of lithium dialkylamides,[5] we paid little attention to the structures or reactivities of the resulting synthetically important lithioimines.[6]

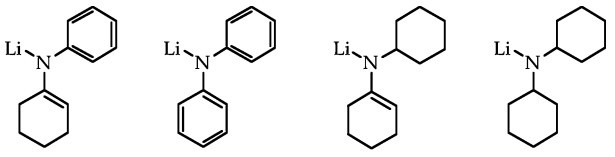

1 **2** **3** **4**

We have now examined structures and alkylations of lithioimine **3** (eq 1). Despite the improved analytical tools, strategies,

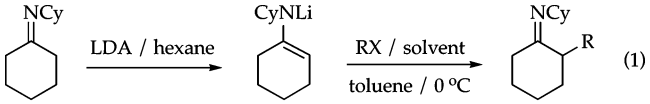

5 **3** **6** (1)

and mechanistic principles acquired during studies of lithium amides, unraveling the structures and reactivities of **3** proved surprisingly challenging. Lithioimine **3** affords a remarkably complex solvent-dependent distribution of monomers, dimers, and trimers. Although careful choice of solvent provides the control over aggregate structure required for mechanistic studies, the complexity resurfaces with a vengeance in an ensemble of monomer- and dimer-based alkylation pathways. Strong evidence suggests that the lithioimine reactants and alkylation transition structures are dominated by competing η^1 (σ-complexed) and η^3 (π-complexed) structural motifs (eq 2).

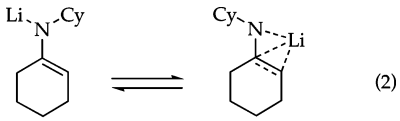

η^1-syn η^3-anti (2)

Results

Throughout the results section we describe solvation and aggregation numbers, rates of exchange, ^{6}Li chemical shifts and ^{6}Li−^{15}N coupling constants, exceptional aggregate stereoselectivities, and inordinate mechanistic complexities. In each case the results are unusual by comparison with their isostructural

(1) (a) Wanat, R. A.; Collum, D. B.; Van Duyne, G.; Clardy, J.; DePue, R. T. *J. Am. Chem. Soc.* **1986**, *108*, 3415. (b) Kallman, N.; Collum, D. B. *J. Am. Chem. Soc.* **1987**, *109*, 7466.
(2) DePue, J. S.; Collum, D. B. *J. Am. Chem. Soc.* **1988**, *110*, 5524.
(3) Aubrecht, K. B.; Collum, D. B. *J. Org. Chem.* **1996**, *61*, 8674.
(4) (a) Zhao, P.; Condo, A.; Keresztes, I.; Collum, D. B. *J. Am. Chem. Soc.* **2004**, *126*, 3113. (b) Wiedemann, S. H.; Ramirez, A.; Collum, D. B. *J. Am. Chem. Soc.* **2003**, *125*, 15893. (c) Sun, X.; Collum, D. B. *J. Am. Chem. Soc.* **2000**, *122*, 2452. (d) Ramirez, A.; Collum, D. B. *J. Am. Chem. Soc.* **1999**, *121*, 11114. (e) Remenar, J. F.; Collum, D. B. *J. Am. Chem. Soc.* **1998**, *120*, 4081. (f) Collum, D. B. *Acc. Chem. Res.* **1993**, *26*, 227. See also refs 2, 5, 9, 11a, and 29.
(5) (a) Liao, S.; Collum, D. B. *J. Am. Chem. Soc.* **2003**, *125*, 15114. (b) Bernstein, M. P.; Collum, D. B. *J. Am. Chem. Soc.* **1993**, *115*, 8008. (c) Bernstein, M. P.; Collum, D. B. *J. Am. Chem. Soc.* **1993**, *115*, 789.
(6) Recent reviews on lithioimines: (a) Mangelinckx, S.; Giubellina, N.; De Kimpe, N. *Chem. Rev.* **2004**, *104*, 2353. (b) Caro, C. F.; Lappert, M. F.; Merle, P. G. *Coord. Chem. Rev.* **2001**, *219*, 605.

Table 1. Stereoselectivity of the Alkylation of Lithioimine **3** with *n*-$C_7H_{15}I$ (eq 1)[a]

entry	solvent	syn/anti[b]
1	THF	10:1
2	THP	>20:1
3	2-MeTHF	>20:1
4	*n*-BuOMe	8:1
5	2,2-Me_2THF	6:1
6	Et_2O	6:1
7	*t*-BuOMe	5:1

[a] Reactions were carried out at −20 °C using 0.1 M solutions of **3** in neat solvent and 1.1 equiv of *n*-$C_7H_{15}I$. Under these conditions, the isomerizations ($t_{1/2}$ > 6 h at 40 °C) proved to be slower than the alkylations. [b] Numerical ratios were obtained from ^{13}C NMR spectra.

lithium dialkylamide counterparts. Analyses of these oddities are placed in the context of computational results that follow. In the interim, aggregation and solvation numbers are described using generic $\mathbf{A}_m\mathbf{S}_n$ designations such that **A** stands for the lithioimine subunit and **S** for solvent.

A. Stereochemistry of Alkylation. Lithioimines alkylate syn to the *N*-alkyl moiety (eq 3),[7] yet the origins of the syn

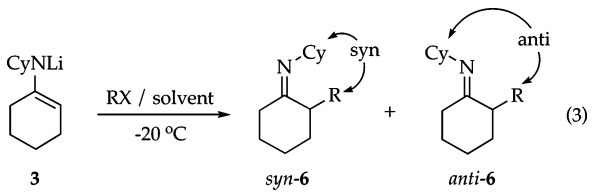

selectivities have been a topic of considerable debate.[8] We examined solvent-dependent syn−anti selectivities by alkylation of lithoimine **3** with 1.1 equiv of *n*-heptyl iodide in neat ethereal solvents at −20 °C (Table 1). The syn and anti orientations in 2-heptyl imine **6** (R = *n*-C_7H_{15}) were assigned using protocols described elsewhere.[5a]

B. NMR Spectroscopic Studies. Lithioimine **3** was isolated as a white solid by treatment of imine **5** with recrystallized[9] lithium diisopropylamide (LDA) in hexane. ^6Li and ^{15}N NMR spectral data[4f,10] derived from solutions of [^6Li,^{15}N]**3** in ethereal solvent/toluene mixtures at −90 °C are summarized in Table 2 and Figures 1−4. Additional spectra are included in the Supporting Information.

Ethereal solvents shown previously to be weakly coordinating ligands for N-lithiated species[11]—*t*-BuOMe, *n*-BuOMe, Et_2O, 2-MeTHF, and 2,2-Me_2THF—each afford a dominant species assigned as a monosolvated dimer $\mathbf{A}_2\mathbf{S}$ along with low concentrations (≤5%) of an isomer (Figure 1). Although the low per-

Table 2. ^6Li and ^{15}N NMR Spectral Data[a]

solvent (S)	structure	compd	^6Li, δ (m, J_{LiN})	^{15}N, δ (m, J_{LiN})
THF	$\mathbf{AS}_{2or3}$	**7**	0.06 (d, 6.8)	143.4 (t, 7.0)
	$\mathbf{A}_3\mathbf{S}_2$	**8**	−0.83[b] (t, 3.4)	125.2 (q, 4.0)
			0.92 (t, 4.8)	131.8 (q, 3.6)
	$\mathbf{A}_2\mathbf{S}$	**11**	1.30 (t, 4.8)	
	$\mathbf{A}_2\mathbf{S}_2$	**12**	0.51 (t, 4.1)	126.2 (br m)
THP	$\mathbf{AS}_{2or3}$	**7**	0.05 (d, 6.8)	141.5 (t, 6.8)
	$\mathbf{A}_3\mathbf{S}_2$	**8**	−0.80[b] (t, 3.8)	124.0 (q, 4.2)
			1.03 (t, 4.6)	131.3 (q, 3.4)
	$\mathbf{A}_2\mathbf{S}$	**11**	1.29 (t, 4.5)	120.9 (q, 4.4)
	$\mathbf{A}_2\mathbf{S}_2$	**12**	0.54 (t, 3.6)	125.0 (q, 3.5)
2-MeTHF	$\mathbf{A}_2\mathbf{S}$[c]	**11**	1.42 (t, 4.4)	119.4 (q, 4.4)
	$\mathbf{A}_2\mathbf{S}$[d]	**10**	0.89 (t, 4.3)	
n-BuOMe	$\mathbf{A}_2\mathbf{S}$[c]	**11**	1.26 (t, 4.4)	118.4 (q, 4.4)
	$\mathbf{A}_2\mathbf{S}$[d]	**10**	0.91 (t, 4.4)	
2,2-Me_2THF	$\mathbf{A}_2\mathbf{S}$	**11**	1.30 (t, 4.4)	119.5 (q, 4.4)
Et_2O	$\mathbf{A}_2\mathbf{S}$[c]	**11**	1.11 (t, 4.4)	119.1 (q, 4.4)
	$\mathbf{A}_2\mathbf{S}$[d]	**10**	0.69 (t, 4.2)	
t-BuOMe	$\mathbf{A}_2\mathbf{S}$	**11**	1.50 (t, 4.3)	118.6 (q, 4.3)

[a] Spectra were recorded on samples containing 0.10 M [^6Li,^{15}N]**3** in excess ethereal solvent. The chemical shifts (δ) are reported relative to that of 0.3 M ^6LiCl/MeOH at −90 °C (0.0 ppm) and neat Me_2NEt (25.7 ppm). Multiplicities are denoted as follows: s = singlet, d = doublet, t = triplet, q = quintet, br m = broad multiplet. Coupling constants were measured after resolution enhancement. All *J* values are reported in Hz. [b] Major resonance (2:1). [c] Major isomer (>20:1). [d] Minor isomer.

lithium solvation number of $\mathbf{A}_2\mathbf{S}$ is foreshadowed by its dominance at well under 1.0 equiv of ethereal ligand per lithium, the structural assignment as a monosolvated dimer derives from studies of strongly coordinating THF (Figure 2) and tetrahydropyran (THP; Figure 3) in which five species coexist: $\mathbf{AS}_{2or3}$, $\mathbf{A}_2\mathbf{S}$ (two isomers), $\mathbf{A}_2\mathbf{S}_2$, and $\mathbf{A}_3\mathbf{S}_2$. The results with THP are slightly cleaner and are presented illustratively as follows.

(1) Definitive assignments for the monomeric and trimeric aggregates are critical to the assignment of the three dimers. Monomer **7** ($\mathbf{AS}_{2or3}$) displays a ^6Li doublet (Figure 3A) and 1:1:1 ^{15}N triplet (Figure 3B) characteristic of a single Li−N contact.[12] The $\mathbf{A}_3\mathbf{S}_2$ trimer is identified by pairs of ^6Li and ^{15}N resonances displaying 2:1 intensities and splitting patterns[13] that, with the aid of single-frequency ^{15}N decoupling (Figure 4), reveal Li−N connectivities (Table 2). The spectroscopic data are consistent with cis,trans stereoisomer **8** rather than cis,cis trimer **9**.

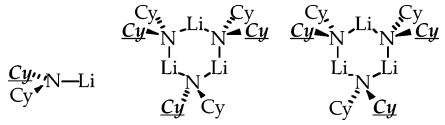

7; $\mathbf{AS}_{2or3}$ **8**; *cis,trans*-$\mathbf{A}_3\mathbf{S}_2$ **9**; *cis,cis*-$\mathbf{A}_3\mathbf{S}_2$

Cy = cyclohexyl; Cy = 1-cyclohexenyl
(solvents not shown)

(2) Having confirmed the structures of the monomer and trimer, we could readily infer the aggregation of the three dimers from lithioimine concentration dependencies showing the relative aggregation numbers:

$$\mathbf{A}_3\mathbf{S}_2 > \mathbf{A}_2\mathbf{S} = \mathbf{A}_2\mathbf{S}_2 > \mathbf{AS}_{2or3}$$

(7) (a) Smith, J. K.; Bergbreiter, D. E.; Newcomb, M. *J. Org. Chem.* **1981**, *46*, 3158. (b) Fraser, R. R.; Banville, J. *J. Chem. Soc., Chem. Commun.* **1979**, 47. (c) Fraser, R. R.; Banville, J.; Dhawan, K. L. *J. Am.* Chem. Soc. **1978**, *100*, 7999. (d) Meyers, A. I.; Williams, D. R.; Erickson, G. W.; White, S.; Druelinger, M. *J. Am. Chem. Soc.* **1981**, *103*, 3081. (e) Meyers, A. I.; Williams, D. R.; Druelinger, M. *J. Am. Chem. Soc.* **1976**, *98*, 3032.
(8) (a) Glaser, R.; Hadad, C. M.; Wiberg, K. B.; Streitwieser, A. *J. Org. Chem.* **1991**, *56*, 6625. (b) Glaser, R.; Streitwieser, A. *J. Org. Chem.* **1991**, *56*, 6612. (c) Fraser, R. R.; Chuaqui-Offermanns, N.; Houk, K. N.; Rondan, N. G. *J. Organomet. Chem.* **1981**, *206*, 131. (d) Houk, K. N.; Strozier, R. W.; Rondan, N. G.; Fraser, R. R.; Chuaqui-Offermanns, N. *J. Am. Chem. Soc.* **1980**, *102*, 1426.
(9) Bernstein, M. P.; Romesberg, F. E.; Fuller, D. J.; Harrison, A. T.; Williard, P. G.; Liu, Q. Y.; Collum, D. B. *J. Am. Chem. Soc.* **1992**, *114*, 5100.
(10) Lucht, B. L.; Collum, D. B. *Acc. Chem. Res.* **1999**, *32*, 1035.
(11) (a) Zhao, P.; Lucht, B. L.; Kenkre, S. L.; Collum, D. B. *J. Org. Chem.* **2004**, *69*, 242. (b) Remenar, J. F.; Lucht, B. L.; Collum, D. B. *J. Am. Chem. Soc.* **1997**, *119*, 5567. (c) Lucht, B. L.; Collum, D. B. *J.* Am. Chem. Soc. **1994**, *116*, 6009. (d) Lucht, B. L.; Collum, D. B. *J. Am. Chem. Soc.* **1995**, *117*, 9863.
(12) The nuclear spins of ^6Li and ^{15}N are 1 and $^1/_2$, respectively.
(13) (a) Gilchrist, J. H.; Harrison, A. T.; Fuller, D. J.; Collum, D. B. *J. Am. Chem. Soc.* **1990**, *112*, 4069. (b) Galiano-Roth, A. S.; Michaelides, E. M.; Collum, D. B. *J. Am. Chem. Soc.* **1988**, *110*, 2658.

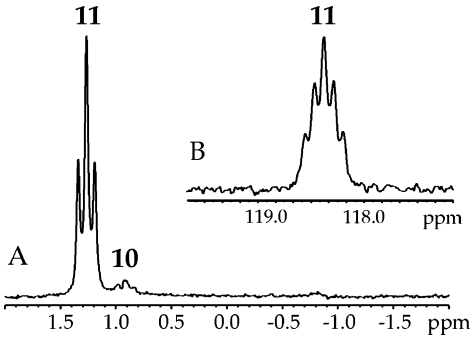

Figure 1. (A) ^{6}Li NMR spectrum of 0.10 M [^{6}Li,^{15}N]**3** in 2.0 M *n*-BuOMe/toluene recorded at −90 °C. (B) ^{15}N NMR spectrum of 0.10 M [^{6}Li,^{15}N]**3** in *n*-BuOMe recorded at −90 °C.

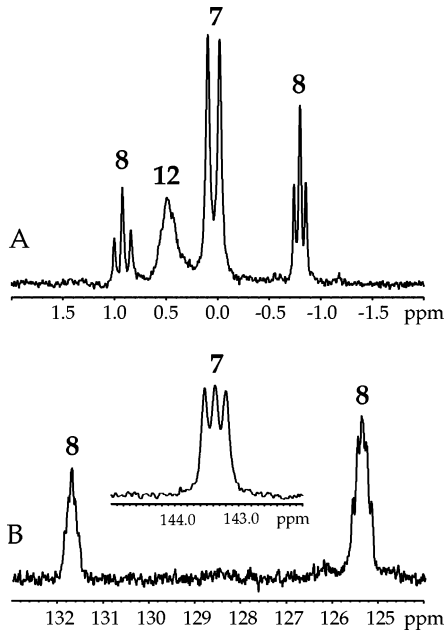

Figure 2. (A) ^{6}Li NMR spectrum of 0.10 M [^{6}Li,^{15}N]**3** in 5.0 M THF/toluene recorded at −90 °C. (B) ^{15}N NMR spectrum of 0.10 M [^{6}Li,^{15}N]**3** in 0.50 M THF/toluene recorded at −90 °C.

(3) Incremental changes in the THP concentration show the relative per-lithium solvation numbers:

$$\mathbf{AS}_{2or3} > \mathbf{A_2S_2} > \mathbf{A_3S_2} > \mathbf{A_2S}$$

The assigned solvation numbers are supported by three observations emanating from the chemistry of lithium amides: (a) trimers are rarely detected in coordinating solvents and are partially solvated (less than one solvent per lithium);[14] (b) monomers are highly solvated (two or more solvents per lithium);[10] and (c) dimers do not exceed one solvent per lithium.[15] The prevalence of the $\mathbf{A_2S}$ form[16] is unusual and receives considerable attention below. Moreover, the incremental changes in THP concentration reveal that the *minor* $\mathbf{A_2S}$ isomer

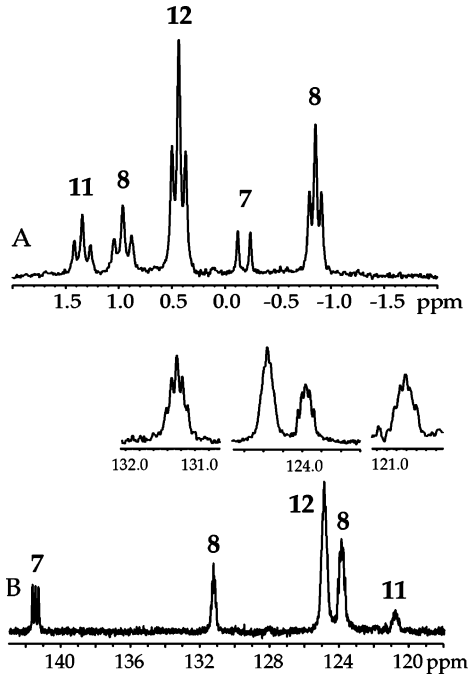

Figure 3. (A) ^{6}Li NMR spectrum of 0.10 M [^{6}Li,^{15}N]**3** in 3.3 M THP/toluene recorded at −90 °C. (B) ^{15}N NMR spectrum of 0.20 M [^{6}Li,^{15}N]**3** in 5.0 M THP/toluene recorded at −90 °C.

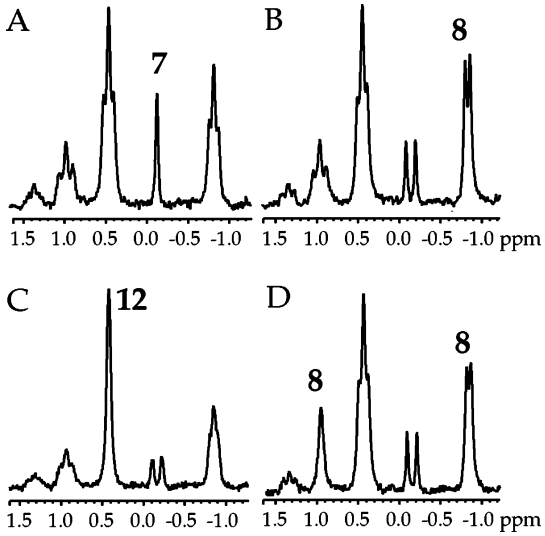

Figure 4. ^{6}Li NMR spectra of 0.20 M [^{6}Li,^{15}N]**3** in 5.0 M THP/toluene recorded at −90 °C with ^{15}N single-frequency decoupling at (A) 142.0 ppm; (B) 131.0 ppm; (C) 125.0 ppm; (D) 124.0 ppm.

is transformed into the sole observable $\mathbf{A_2S_2}$ form with concomitant disappearance of the *major* $\mathbf{A_2S}$ isomer.[17]

(4) We assign the isomeric $\mathbf{A_2S}$ dimers as trans (**10**) and cis (**11**). Such stereoisomerism is observed in the slow exchange

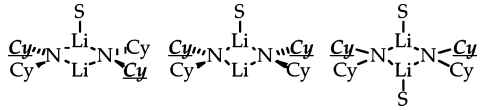

10; *trans*-$\mathbf{A_2S}$ **11**; *cis*-$\mathbf{A_2S}$ **12**; $\mathbf{A_2S_2}$ (one isomer)

(14) (a) Rutherford, J. L.; Collum, D. B. *J. Am. Chem. Soc.* **2001**, *123*, 199. (b) Rutherford, J. L.; Collum, D. B. *J. Am. Chem. Soc.* **1999**, *121*, 10198.

(15) (a) Williard, P. G.; Salvino, J. M. *J. Org. Chem.* **1993**, *58*, 1. (b) DePue, J. S.; Collum, D. B. *J. Am. Chem. Soc.* **1988**, *110*, 5518. (c) Jackman, L. M.; Scarmoutzos, L. M.; DeBrosse, C. W. *J. Am. Chem. Soc.* **1987**, *109*, 5355. (d) Setzer, W. N.; Schleyer, P. v. R. *Adv. Organomet. Chem.* **1985**, *24*, 354. (e) Lappert, M. F.; Slade, M. J.; Atwood, J. L.; Rogers, R. D.; Shakir, R. *J. Am. Chem. Soc.* **1983**, *105*, 302. See also ref 1b.

(16) $\mathbf{A_2S}$ cyclic dimers of simple lithium dialkylamides in solution have been reported: (a) Lucht, B. L.; Bernstein, M. P.; Remenar, J. F.; Collum, D. B. *J. Am. Chem. Soc.* **1996**, *118*, 10707. (b) Lucht, B. L.; Collum, D. B *J. Am. Chem. Soc.* **1996**, *118*, 2217. See also ref 11d.

(17) The conversion of the minor $\mathbf{A_2S}$ form to the major $\mathbf{A_2S_2}$ occurs with a marked THP-concentration-dependent migration characteristic of rapid solvent exchange.

limit in the trimer (above) as well as in dimeric lithium amides.[13b] Can we rule out alternative forms of isomerism attributable to the location of the solvent or π complexation? We think so. Each of the two $\mathbf{A}_2\mathbf{S}$ isomers necessarily contains two magnetically inequivalent ^{6}Li nuclei, yet they appear symmetric in the low-temperature limit consistent with the rapid solvent exchange observed in many hindered lithium amides.[4f] Similarly, the conversion of the minor $\mathbf{A}_2\mathbf{S}$ form to the major $\mathbf{A}_2\mathbf{S}_2$ form occurs under conditions of rapid solvent exchange.[17] Computational studies described below confirm that solvent exchange and $\eta^1-\eta^3$ isomerization should both be facile. The apparent high and opposite stereoselectivities for the $\mathbf{A}_2\mathbf{S}$ and $\mathbf{A}_2\mathbf{S}_2$ dimers ($\geq$20:1) are surprising.

(5) The structural diversity of lithioimine **3** is accompanied by a large chemical shift dispersion in the ^{6}Li NMR spectra and by unprecedented variations in the coupling constants of the dimers and within the trimer (Table 2). The influence of both solvation and π complexation are discussed below.

C. Calculated Reactant Structures. We turned to density functional theory (DFT) calculations at the B3LYP/6-31G(d) level[18] to investigate contributions of η^1 and η^3 hapticities to the solution structures of lithioimine **3**. Gibbs free energies (ΔG^0, kcal/mol) include thermal corrections at 298.15 K. Lithioimine **3** and ethereal solvents were modeled using the lithiated *N*-isopropylimine of acetone (**13**) and Me_2O, respectively. We considered all reasonable permutations of imine stereoisomers (syn vs anti; eq 4), solvation and aggregation numbers (eq 5), hapticities (η^1 vs η^3; eq 6), and aggregate stereoisomers (cis vs trans; eq 7). Most of the results are archived in the Supporting Information. We occasionally refer to relative stabilities or energies: these statements are implicitly based on the requisite balanced equilibria. A few selected results are summarized as follows.

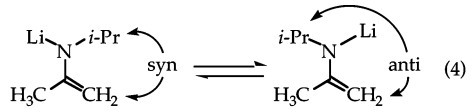

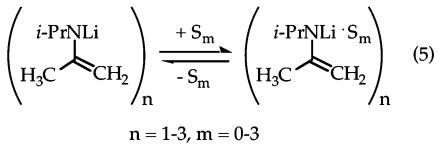

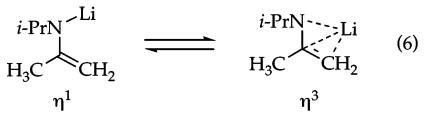

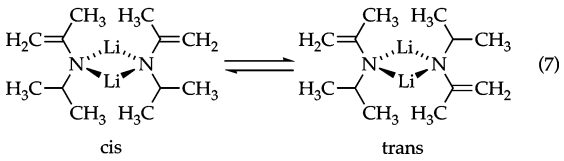

(18) All calculations were executed using *Gaussian 03*, revision B.04; Gaussian, Inc.: Pittsburgh, PA, 2003. See the Supporting Information for the full list of authors.

Chart 1. Relative Free Energies of the Optimized Structures for the Serial Solvation of Lithioimine **13**

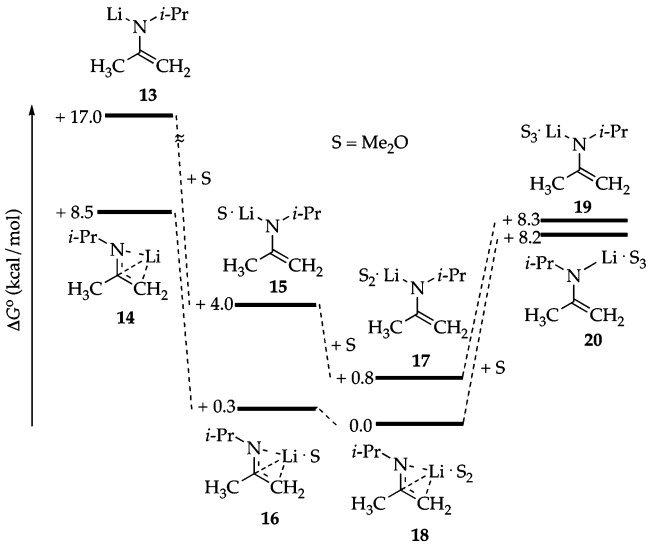

complex containing two solvents (**18**) followed closely by the corresponding monosolvate **16** (Chart 1). The π interaction readily found in the anti isomers is *incompatible* with the syn orientation. The non-π-complexed disolvate is predicted to be more stable in the syn orientation (**17**).[19] The correlation of anti with η^3 and syn with η^1 (eq 2) shows up again in the context of the dimers (below).[8a,20] All forms of the trisolvate are highly destabilized.

To understand the considerable and unexpected variations in both ^{6}Li chemical shifts and ^{6}Li$-^{15}$N coupling constants we turned to GIAO (gauge-independent atomic orbitals) [21] and DFT calculations.[22] Monomers of N-lithiated species routinely show large coupling constants.[4f] They offer a logical starting point to consider how solvation and π complexation influence coupling constants and chemical shifts. In short, the calculations predict that π complexation in the $\mathbf{AS}_n$ monomers decreases the absolute $J_{\mathrm{Li-N}}$ values by 3$-$5 Hz[23] but has little influence on the ^{6}Li chemical shifts.

C.2. Dimers. Of the eight possible unsolvated dimers, trans isomer **21** and cis isomer **22** are the most stable (Chart 2). In general, cis and trans isomers about the Li_2N_2 ring are of nearly equal energy, and π interactions are stabilizing by 4$-$5 kcal/mol each. As found with the monomers, the anti *N*-alkyl orientation (eq 4) is affiliated exclusively with the π complexation, whereas the syn orientation is affiliated exclusively with the η^1 motif.

(19) Ab initio calculations on unsolvated lithioimines: (a) Pratt, L. M.; Khan, I. M. *J. Mol. Struct.* **1996**, *367*, 33. (b) Pratt, L. M.; Hogen-Esch, T. E.; Khan, I. M. *Tetrahedron* **1995**, *51*, 5955.

(20) For X-ray structures of monomeric azaallyllithiums, see: (a) Hitchcock, P. B.; Lappert, M. F.; Layh, M.; Liu, D.-S.; Sablong, R.; Shun, T. *J. Chem. Soc., Dalton Trans.* **2000**, 2301. (b) Hitchcock, P. B.; Lappert, M. F.; Leung, W.-P.; Liu, D.-S.; Mak, T. C. W.; Wang, Z.-X. *J. Chem. Soc., Dalton Trans.* **1999**, 1263. (c) Colgan, D.; Papasergio, R. I.; Raston, C. L.; White, A. H. *J. Chem. Soc., Chem. Commun.* **1984**, 1708.

(21) Wolinski, K.; Hilton, J. F.; Pulay, P. *J. Am. Chem. Soc.* **1990**, *112*, 8251 and references therein.

(22) For theoretical investigations of ^{6}Li$-^{15}$N coupling constants, see: (a) Parisel, O.; Fressigné, C.; Maddaluno, J.; Giessner-Prettre, C. *J. Org. Chem.* **2003**, *68*, 1290. (b) Koizumi, T.; Morihashi, K.; Kikuchi, O. *Bull. Chem. Soc. Jpn.* **1996**, *69*, 305.

(23) Differences in coupling constants to N have been rationalized in terms of changes in hybridization: Schulman, J. M.; Venanzi, T. *J. Am. Chem. Soc.* **1976**, *98*, 4701.

Chart 2

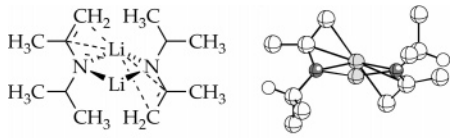

21
ΔG^o = 0.0 kcal

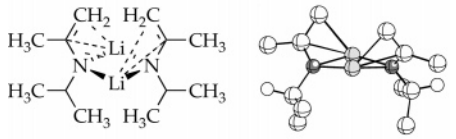

22
ΔG^o = - 0.2 kcal

Among the disolvated dimers, trans isomer **23** displaying both π interactions *and* solvation on each lithium is the most stable. The solvation of dimer **21**, which bears geminal π interactions, affords vicinal π complex **23** with a net stabilization of >5 kcal/mol. In contrast, solvation of cis isomer **22** to give **24** involves the loss of one π interaction and is destabilizing by >1 kcal/mol. The most stable cis isomer corresponds to dimer **25**, which bears a syn *N*-alkyl group and a single π interaction. It is interesting that trans isomer **23** is more stable than cis isomers **24** and **25** because we argue that the monosolvated dimer ($\mathbf{A_2S}$) and the disolvated dimer ($\mathbf{A_2S_2}$) are of opposite stereochemistries. Therefore, it was gratifying to find that a crystal structure of lithioimine **3** obtained from Me_2NEt/pentane reveals an $\mathbf{A_2S_2}$ trans isomer akin to **23** (Figure 5).[24,25]

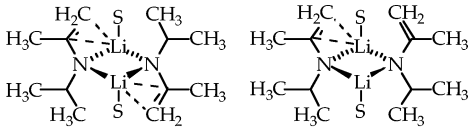

23
ΔG^o = - 5.2 kcal

24
ΔG^o = + 1.3 kcal

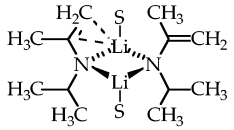

25
ΔG^o = - 3.3 kcal

The monosolvated dimers ($\mathbf{A_2S}$) were particularly interesting owing to their unanticipated stability we detected spectroscopically. The calculations suggest that the monosolvate corresponds to trans isomer **26**, which bears geminal π interactions. We suspect, however, that the simplified model may be underestimating the steric demands on the experimentally observed lithioimine **3**,[19] and we consider the less stable cis isomer **27** and its mono-π-complexed form **28** as viable alternatives despite their predicted lower stability.

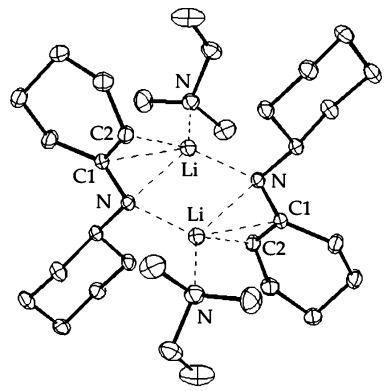

Figure 5. Ortep drawing of lithioimine trans isomer of **12** ($\mathbf{A_2S_2}$, **S** = Me_2EtN).

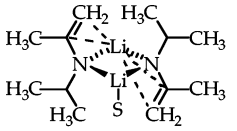

26
ΔG^o = - 3.6 kcal

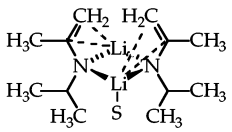

27
ΔG^o = - 0.5 kcal

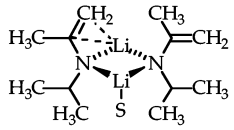

28
ΔG^o = + 0.8 kcal

GIAO and spin−spin coupling calculations on the dimers presented a very complex problem. The dimers contain either one or two distinct lithiums and as many as four distinct Li−N bonds. Conversely, the spectroscopy records the time-averages. Accordingly, we pooled the results by defining four substructures—$\mathbf{A}(\eta^1)$, $\mathbf{AS}(\eta^1)$, $\mathbf{A}(\eta^3)$, and $\mathbf{AS}(\eta^3)$—found in the various $\mathbf{A_2}$, $\mathbf{A_2S}$, and $\mathbf{A_2S_2}$ dimers and by simply averaging the relative chemical shifts ($\Delta\delta$) and coupling constants (ΔJ, Scheme 1). We find that solvation has little effect on the coupling constants. Solvation reduces the chemical shift, but only for the π-complexed forms [cf., $\mathbf{A}(\eta^3)$ and $\mathbf{AS}(\eta^3)$]. By contrast, π complexation markedly reduces the coupling constant and chemical shift in both the unsolvated and the solvated forms (consistent with results from studies of the monomers). The calculated spectroscopic properties do not offer refinements to the observed structural forms per se, but they do suggest that solvation and π complexation can account for the variations in ^{6}Li chemical shift and ^{6}Li−^{15}N coupling observed for $\mathbf{A_2S}$ and $\mathbf{A_2S_2}$.[14a,26]

C.3. Trimers. The structural variations in the trimer impart a complexity that limited the scope of the computational study,

(24) The key structural data for the crystal structure of lithioimine **3** are located in the Supporting Information and have been archived in the Cambridge Crystallographic Database (CCDC 287980).

(25) Other X-ray structures of dimeric azaallyllithiums include the following. (i) Bis-η^1 disolvated: (a) Armstrong, D. R.; Clegg, W.; Dunbar, L.; Liddle, S. T.; MacGregor, M.; Mulvey, R. E.; Reed, D.; Quinn, S. A. *J. Chem. Soc., Dalton Trans.* **1998**, 3431. See also ref 1a. (ii) Bis-η^3 disolvated: (b) Boyd, C. L.; Tyrrell, B. R.; Mountford, P. *Acta Crystallogr., Sect. E: Struct. Rep. Online* **2002**, *58*, m597. (c) Knorr, R.; Dietrich, H.; Mahdi, W. *Chem. Ber.* **1991**, *124*, 2057. (d) Engelhardt, L. M.; Jacobsen, G. E.; Junk, P. C.; Raston, C. L.; Skelton, B. W.; White, A. H. *J. Chem. Soc., Dalton Trans.* **1988**, 1011. (e) Jackman, L. M.; Scarmoutzos, L. M.; Smith, B. D.; Williard, P. G. *J. Am. Chem. Soc.* **1988**, *110*, 6058. (f) Dietrich, H.; Mahdi, W.; Knorr, R. *J.* Am. Chem. Soc. **1986**, *108*, 2462. (g) Colgan, D.; Papasergio, R. I.; Raston, C. L.; White, A. H. *J. Chem. Soc., Chem. Commun.* **1984**, 1708. (iii) Bis-η^3 unsolvated internal chelate: (h) Polt, R. L.; Stork, G.; Carpenter, G. B.; Williard, P. G. *J. Am. Chem. Soc.* **1984**, *106*, 4276. (iv) Bis-η^3 unsolvated: (i) Hitchcock, P. B.; Lappert, M. F.; Liu, D.-S. *J. Chem. Soc., Chem. Commun.* **1994**, 2637. See also ref 20c. (v) Bis-η^1 unsolvated internal chelate: (j) Antolini, F.; Gehrhus, B.; Hitchcock, P. B.; Lappert, M. F. *Angew. Chem. Int. Ed.* **2002**, *41*, 2568.

(26) For experimental differences in ^{6}Li−^{15}N coupling constants upon changes in Li coordination, see: Arvidsson, P.; Davidsson, Ö. *Angew. Chem., Int. Ed. Engl.* **2000**, *39*, 1467 and references therein.

Scheme 1. Effect of Solvation and π Complexation upon Calculated Chemical Shifts (δ, ppm) and Coupling Constants (J, Hz) for Dimers $\mathbf{A}_2\mathbf{S}_n$

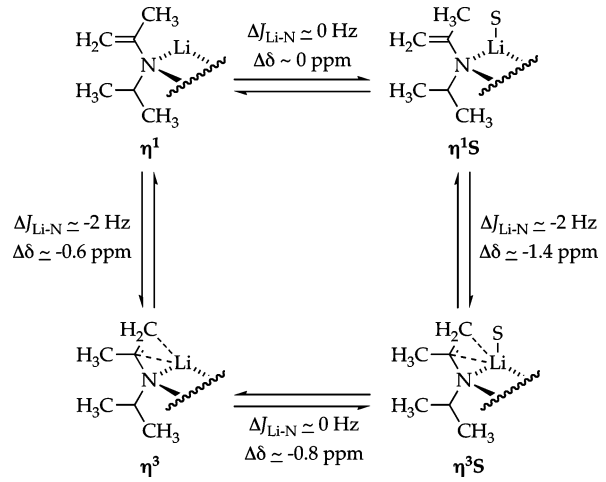

but several trends are notable. The most stable form is **29** corresponding to unsolvated trimer $\mathbf{A}_3$,[27] but monosolvated trimer **30** and disolvated trimer **31** corresponding to $\mathbf{A}_3\mathbf{S}$ and $\mathbf{A}_3\mathbf{S}_2$, respectively, are only a few kcal/mol less stable. π interactions are prominent and stabilizing. The cis,trans isomers (corresponding to cis,trans isomer **8**) are considerably more stable (>5 kcal/mol) than the cis,cis isomers (corresponding to cis,cis isomer **9**) as observed experimentally. The trisolvated trimers ($\mathbf{A}_3\mathbf{S}_3$) are substantially less stable (>6 kcal/mol). Last, calculated ^{6}Li chemical shifts and ^{6}Li−^{15}N coupling constants show sensitivities to π complexation and solvation similar to those noted for the dimers.

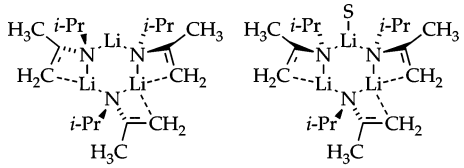

29
ΔG = 0.0 kcal

30
ΔG = + 2.1 kcal

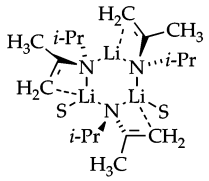

31
ΔG = + 2.3 kcal

D. Kinetics of Alkylation. Solution kinetics were carried out using *n*-BuOMe, 2-MeTHF, *t*-BuOMe, and Et_2O—solvents affording monosolvated dimers ($\mathbf{A}_2\mathbf{S}$) as the sole observable forms. Lithioimine **3** was alkylated at 0 °C using *n*-$C_7H_{15}I$

Table 3. Summary of Rate Studies for the Alkylation of **3** at 0 °C (eq 1)

entry	solvent (S)	RX	S order	**3** order at indicated [S]	
1	*n*-BuOMe	*n*-$C_7H_{15}I$	0.90 ± 0.09; 0	0.92 ± 0.02	(2.10 M)
2	*n*-BuOMe	*n*-$C_7H_{15}I$		0.84 ± 0.04	(6.10 M)
3	2-MeTHF	*n*-$C_7H_{15}I$	1.60 ± 0.09; 0		
4	2-MeTHF	*n*-$C_8H_{17}Br$	1.78 ± 0.02; 0	0.61 ± 0.02	(1.10 M)
5	2-MeTHF	*n*-$C_8H_{17}Br$		0.62 ± 0.01	(4.10 M)
6	2-MeTHF	*n*-$C_8H_{17}Br$		0.68 ± 0.02	(8.10 M)
7	*t*-BuOMe	*n*-$C_7H_{15}I$	1; 0	0.81 ± 0.02	(2.10 M)
8	*t*-BuOMe	*n*-$C_7H_{15}I$		0.64 ± 0.04	(6.10 M)
9	Et_2O	*n*-$C_7H_{15}I$		0.73 ± 0.03	(2.10 M)
10	Et_2O	*n*-$C_7H_{15}I$	0.65 ± 0.03	0.69 ± 0.03	(8.10 M)

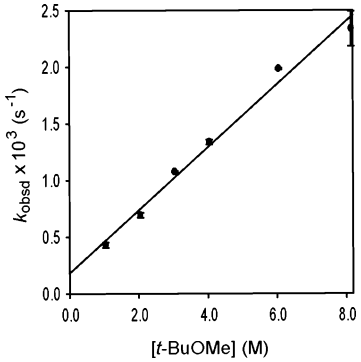

Figure 6. Plot of k_{obsd} vs [*t*-BuOMe] in toluene cosolvent for the alkylation of **3** (0.10 M) with *n*-$C_7H_{15}I$ (0.005 M) at 0 °C. The curve depicts an unweighted least-squares fit to $k_{obsd} = a + b$[*t*-BuOMe] ($a = 0.18 \pm 0.06$, $b = 0.28 \pm 0.01$).

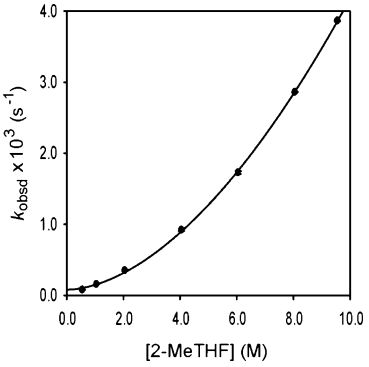

Figure 7. Plot of k_{obsd} vs [2-MeTHF] in toluene cosolvent for the alkylation of **3** (0.10 M) with *n*-$C_8H_{17}Br$ (0.005 M) at 0 °C. The curve depicts an unweighted least-squares fit to $k_{obsd} = a + b$[2-MeTHF]^c ($a = 0.08 \pm 0.01$, $b = 0.068 \pm 0.003$, $c = 1.78 \pm 0.02$).

for the less reactive lithioimine/solvent combinations and *n*-$C_8H_{17}Br$ for the more reactive combinations ($k_{RI}/k_{RBr} = 33 \pm 1$ in 1.1 M 2-MeTHF). Pseudo-first-order conditions were established with **3** at normal concentrations (0.05−0.50 M) by restricting the alkyl halide concentration to ≤0.005 M.[28] The reaction rates were monitored by following the loss of the alkyl halide in quenched samples via gas chromatographic analysis.[29] Clean first-order decays were observed to 4−5 half-lives and afforded pseudo-first-order rate constants (k_{obsd}). The results of the rate studies are summarized in Table 3. Representative rate data are depicted in Figures 6−9; additional data are included in the Supporting Information.

(27) X-ray structures of unsolvated $(R_2NLi)_3$ trimers include the following. (i) *cis,trans*-Tris-η^3 lithioimine: (a) Antiñolo, A.; Huertas, C.; del Hierro, I.; Lappert, M. F.; Otero, A.; Prashar, S.; Rodriguez, A. M.; Villaseñor, E. *Organometallics* **1998**, *17*, 5874. (ii) *cis,cis-vic*-Tris-η^3 lithioimine: (b) Hitchcock, P. B.; Lappert, M. F.; Wei, X.-H. *J. Organomet. Chem.* **2003**, *683*, 83. (iii) *cis,trans*-Lithium amide: (c) Gemund, B.; Nöth, H.; Sachdev, H.; Schmidt, M. *Chem. Ber.* **1996**, *129*, 1335. (iv) *cis,cis*-Lithium amide: (d) Wrackmeyer, B.; Schwarze, B.; Weidinger, J.; Milius, W. *Z. Naturforsch., B: Chem. Sci.* **1997**, *52*, 431. (e) Armstrong, D. R.; Baker, D. R.; Craig, F. J.; Mulvey, R. E.; Clegg, W.; Horsburgh, L. *Polyhedron* **1996**, *15*, 2533.

(28) [**3**] refers to the formal molarity of the monomer unit (normality). The solvent concentration refers to the total concentration of donor solvent (free and lithium-bound) in toluene cosolvent unless stated otherwise.

(29) (a) Remenar, J. F.; Collum, D. B. *J. Am. Chem. Soc.* **1997**, *119*, 5573. (b) Remenar, J. F.; Collum, D. B. *J. Am. Chem. Soc.* **1998**, *120*, 4081.

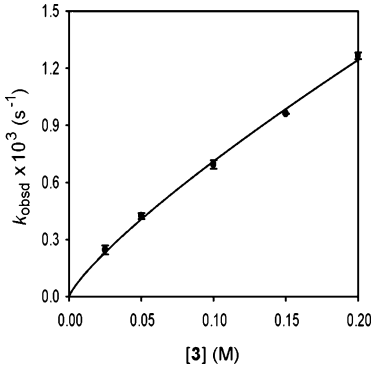

Figure 8. Plot of k_{obsd} vs [**3**] in 2.10 M *t*-BuOMe and toluene cosolvent for the alkylation of **3** with *n*-$C_7H_{15}I$ (0.005 M) at 0 °C. The curve depicts an unweighted least-squares fit to $k_{obsd} = a[\mathbf{3}]^b$ ($a = 4.5 \pm 0.2$, $b = 0.81 \pm 0.02$).

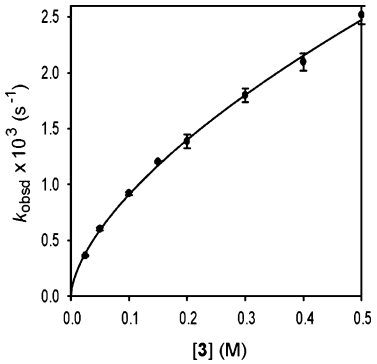

Figure 9. Plot of k_{obsd} vs [**3**] in 4.10 M 2-MeTHF and toluene cosolvent for the alkylation of **3** with *n*-$C_8H_{17}Br$ (0.005 M) at 0 °C. The curve depicts an unweighted least-squares fit to $k_{obsd} = a[\mathbf{3}]^b$ ($a = 3.8 \pm 0.1$, $b = 0.62 \pm 0.01$).

Table 4. Relative Rate Constants (k_{rel}) for the Alkylation of **3** (0.10 M) with *n*-$C_7H_{15}I$ (0.005 M) in 1.10 M Solvent/Toluene Mixtures at 0 °C (eq 1)

entry	solvent (S)	k_{rel}
1	THF	60
2	THP	10
3	2-MeTHF	14
4	*n*-BuOMe	1.0
5	Et_2O	1.0
6	*t*-BuOMe	1.2

D.1. Solvent-Dependent Relative Rates. We provide a selection of solvent-dependent relative rate constants as a preface to the rate studies (Table 4). On the basis of binding constants measured on dimeric lithium amides,[11b,d] the rates qualitatively correlate with solvation energies. The rate constants also qualitatively correlate with the tendency to form monomer (although causal relationships between aggregation and reactivity are often overstated).[30]

D.2. Idealized Rate Laws. The results and discussion are presented in the context of possible monomer- and dimer-based mechanisms summarized in eqs 8−14. All the listed mechanisms have precedent from rate studies of lithium amides.[4] Although fractional organolithium orders are emblematic of mechanisms requiring deaggregation, fractional solvent orders (eqs 8−10) are peculiar consequences of the partial solvation of the starting $\mathbf{A_2S}$ dimer.

(30) Collum, D. B. *Acc. Chem. Res.* **1992**, *25*, 448.

Monomer-based pathways:

$$0.5\mathbf{A_2S} + 0.5\mathrm{S} + \mathrm{RX} \rightarrow [\mathbf{AS}(\mathrm{RX})]^{\ddagger} \quad (8)$$

$$0.5\mathbf{A_2S} + 1.5\mathrm{S} + \mathrm{RX} \rightarrow [\mathbf{AS_2}(\mathrm{RX})]^{\ddagger} \quad (9)$$

$$0.5\mathbf{A_2S} + 2.5\mathrm{S} + \mathrm{RX} \rightarrow [\mathbf{AS_3}(\mathrm{RX})]^{\ddagger} \quad (10)$$

Dimer-based pathways:

$$\mathbf{A_2S} + \mathrm{RX} \rightarrow [\mathbf{A_2S}(\mathrm{RX})]^{\ddagger} \quad (11)$$

$$\mathbf{A_2S} + \mathrm{S} + \mathrm{RX} \rightarrow [\mathbf{A_2S_2}(\mathrm{RX})]^{\ddagger} \quad (12)$$

$$\mathbf{A_2S} + 2\mathrm{S} + \mathrm{RX} \rightarrow [\mathbf{A_2S_3}(\mathrm{RX})]^{\ddagger} \quad (13)$$

$$\mathbf{A_2S} + 3\mathrm{S} + \mathrm{RX} \rightarrow [\mathbf{A_2S_4}(\mathrm{RX})]^{\ddagger} \quad (14)$$

D.3. Reaction Order in Solvent. A plot of k_{obsd} versus *t*-BuOMe concentration for the alkylation of **3** with *n*-$C_7H_{15}I$ shows an approximate first-order dependence on *t*-BuOMe[31] with a minor, but potentially significant, nonzero intercept (Figure 6). Although a plot of k_{obsd} versus *n*-BuOMe concentration shows similar effects, a more broadly based survey of solvent orders reveals a very complex picture. A plot of k_{obsd} versus Et_2O concentration displays a distinct downward curvature (Table 3) that is neither a half-order, emblematic of the monomer-based reactions (eqs 8−10), nor an integer value representative of dimer-based reactions (eqs 11−14). Conversely, a plot of k_{obsd} versus 2-MeTHF shows a distinct exponential dependence (Figure 7) that is halfway between 1.5, expected for a disolvated monomer (eq 9), and 2.0, anticipated for a trisolvated dimer (eq 13). Leaving the error bars aside—error bars do not attest to systematic error—we turn to personal experience with rate studies of lithium amides[4] and note that these deviations of the reaction order in solvent from idealized values are abnormally large.

D.4. Reaction Order in Lithioimine. A plot of k_{obsd} versus concentration of **3** at low *t*-BuOMe concentration visually approximates linearity, but the measured order of 0.81 ± 0.02 represents a substantial deviation from either 0.5 or 1.0, characteristic of monomer- or dimer-based reactions, respectively (Figure 8). Similarly, a plot of k_{obsd} versus concentration of **3** at low 2-MeTHF concentration clearly displays the curvature anticipated for a fractional order, yet the measured order of 0.62 ± 0.01 again constitutes a significant deviation from 0.5 (Figure 9). Moreover, changing the solvent concentrations causes unpredictable variations in the lithioimine orders. Inspection of the measured orders in Table 3 reveals that the reaction orders are intermediate values for all solvents under all conditions. These large variations in reaction orders are simply not observed during rate studies of lithium dialkylamides. We discuss the origins of these contrasting behaviors below.

E. Calculated Transition Structures. Transition structures for monomer- and dimer-based alkylations were calculated using the methods described above.[18,32] Methyl bromide was used as a model for the alkylating agents. In each case, the calculated

(31) Alternatively, an unweighted least-squares fit to $k_{obsd} = a[\mathbf{3}]^b + c$ affords the following: $a = 0.6 \pm 0.2$, $b = 0.7 \pm 0.1$, $c = -0.2 \pm 0.2$.
(32) The Ahlrichs all-electron SVP basis set was used for Br, and 6-31G(d) was used for the remaining atoms.

Chart 3

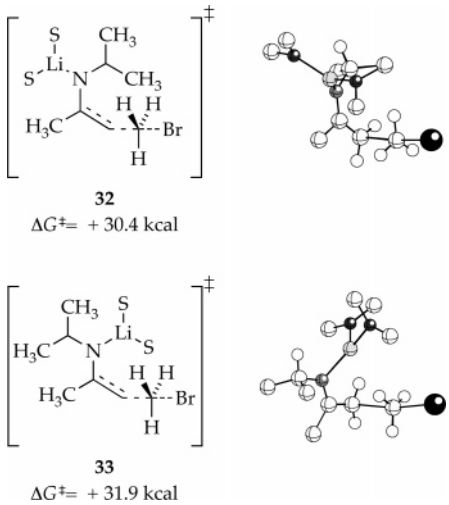

32
$\Delta G^{\ddagger}$= + 30.4 kcal

33
$\Delta G^{\ddagger}$= + 31.9 kcal

Chart 4

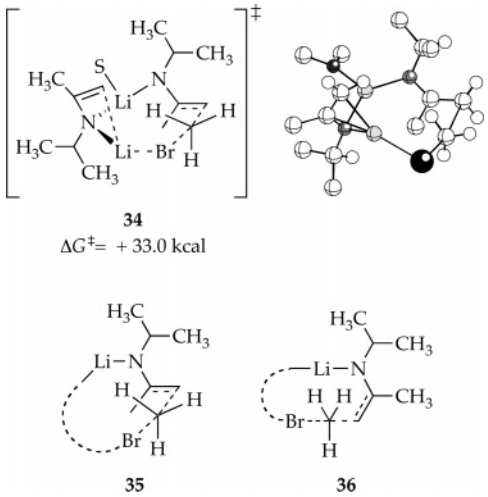

34
$\Delta G^{\ddagger}$= + 33.0 kcal

35 **36**

transition structures were shown to be legitimate saddle points by the existence of a single imaginary frequency. The energies are arbitrarily related to monosolvated dimeric reactant **27**.

E.1. Monomers. The most prominent feature of the monomer-based alkylations is the absence of π complexation in the transition structures (Chart 3). Moreover, the transition structures mirror the reactants in that the disolvated monomers are preferred, whereas the trisolvated monomers are relatively unstable. The often cited preference for syn alkylation is also supported: transition structure **32**, displaying a syn oriented *N*-alkyl moiety, is the most stable. Anti oriented transition structure **33** is also viable but is less stable than **32**. Li−Br interactions do not appear to be geometrically feasible.[33]

E.2. Dimers. Calculated dimer-based transition structures show some very curious structural details (Charts 4 and 5). Overall, the most stable dimer-based transition structure, **34**, is only 2−3 kcal/mol less stable than the monomer-based variants. Transition structure **34** is a medium ring with an endocyclic Li−Br interaction. One lithium is solvated, whereas the ancillary lithioimine unit (the unit not directly involved in the alkylation) is π complexed. Dimer **34** displays the experimentally observed

Chart 5

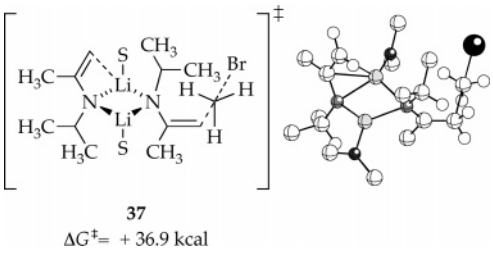

37
$\Delta G^{\ddagger}$= + 36.9 kcal

syn orientation about the imine group (eq 4). No anti oriented alkylations were detected for medium-sized cyclic transition structures. This preference for cyclic transition structures with a syn orientation requiring a 180° Li−N−C−C dihedral angle (**35**) instead of transition structures with an anti orientation requiring a 0° Li−N−C−C dihedral angle (**36**) seems counter-intuitive on first inspection.[34]

Viable disolvated dimer-based transition structures could be found but were decidedly less stable than **34**. The second solvent induces a strong preference for a four-membered Li_2N_2 dimer structure (Chart 5) with exocyclic alkylation (**37**) rather than the medium-sized ring preferred by the monosolvates. Transition structures bearing syn or anti orientations on the *ancillary* lithioimine in the four-membered dimers are of approximately equal energy.

There are several noteworthy general patterns. Under no circumstances could transition structures be found in which the lithioimine undergoing alkylation contained a π-complexed lithium. This result is consistent with those from the monomer-based transition structures. In contrast, π complexation in the ancillary imine is clearly a dominant structural motif. Also, the ancillary lithioimine subunit displays a clear correlation between η^1-syn and η^3-anti, as found in the reactants.

Discussion

It is clear that *N*-alkyllithioimines are *not* simply vinylogous analogues of lithium dialkylamides. In virtually every facet of the chemistry of lithioimine **3**, we observed behaviors that diverge from those of isostructural lithium dialkylamides and a concomitant increase in complexity. These differences are attributed to the intervention of η^3 (π) complexation (eq 6).

Aggregation and Solvation Number. Whereas lithium dialkylamides exemplified by LDA (or lithium dicyclohexylamide, **4**) routinely form disolvated dimers over a range of conditions, lithioimine **3** in strongly coordinating ligands (THF and THP) shows a penchant to form highly solvated monomers ($\mathbf{AS}_{2or3}$), monosolvated dimers ($\mathbf{A}_2\mathbf{S}$; two isomers), and disolvated trimers ($\mathbf{A}_3\mathbf{S}_2$) in addition to the anticipated disolvated dimers ($\mathbf{A}_2\mathbf{S}_2$). The appearance of the monomer is consistent with a charge-stabilized lithium amide.[2,15b] By contrast, the marked stability of monosolvated dimer $\mathbf{A}_2\mathbf{S}$ and the persistence of the trimer even at elevated solvent concentrations have no precedents in the chemistry of lithium dialkylamides. Lithioimine **3** solvated by slightly weaker ligands—*n*-BuOMe, *t*-BuOMe, Et_2O, 2-MeTHF, and 2,2-Me_2THF—forms exclusively a pair of isomeric $\mathbf{A}_2\mathbf{S}$ dimers rather than the anticipated $\mathbf{A}_2\mathbf{S}_2$ dimers.

(33) Calculations on the alkylation of a lithium enolate with MeBr show the absence of Li−Br contacts in exo transition structures: Ikuta, Y.; Tomoda, S. *Org. Lett.* **2004**, *6*, 189.

(34) For a discussion on the conformation of medium-sized cyclenes, see: Buemi, G.; Favini, G.; Zuccarello, F. *J. Mol. Struct.* **1996**, *367*, 33.

Isomerism. Solvent−solvent exchanges on the various aggregates of **3** are very rapid. Consequently, aggregates differing only in number or position of solvents do *not* add to or explain the spectral complexity. Similarly, spectroscopic and computational data strongly suggest that $\eta^1-\eta^3$ exchanges are also rapid on the NMR time scales. In contrast, evidence of slow exchange of stereoisomers about the Li_nN_n rings (eq 7) is well founded in the chemistry of lithium amides[13b] and is consistent with our experimental observations. Nonetheless, the degree of stereocontrol is surprising. The $\mathbf{A_3S_2}$ trimer is exclusively cis,trans trimer **8**. The $\mathbf{A_2S}$ dimers are assigned as a 20:1 cis,trans (or trans,cis) mixture corresponding to **10** and **11**. The sole observable $\mathbf{A_2S_2}$ dimer corresponds to a disolvated version of the *minor* $\mathbf{A_2S}$ stereoisomer.[17]

DFT computations show a modest bias for π-complexed forms. More to the point, however, a large number of monomers, dimers, and trimers with both η^1- and η^3-complexed lithioimine subunits are viable within a reasonably narrow range of energies. The computations provide a definitive prediction about the relationship of hapticity and syn−anti isomerism: η^3 complexation is affiliated exclusively with the anti oriented *N*-alkyl substituent, whereas η^1 complexation is affiliated with the syn oriented form (eq 2).[8a,20] This relationship holds regardless of aggregation state and is important mechanistically, as discussed shortly. The computations also suggest that the surprising variations in the $^6Li-^{15}N$ couplings derive from attenuated coupling by π-complexed lithiums.

Mechanism of Lithioimine Alkylation. Rate studies of the C-alkylation of lithioimine **3** were carried out using four solvents that afford $\mathbf{A_2S}$ dimers as the sole observable forms. Despite the critical success at controlling the structure of **3**, the complexity resurfaces in the context of the rate studies: reaction orders in lithioimine **3** and donor solvent (Table 3) are intermediate between those anticipated for monomer-based (eqs 8−10) and dimer-based alkylations (eqs 11−14). Taken together, the rate laws suggest a chronic superposition of mechanisms.

Computations provide a partial explanation for the mechanistic complexity and offer provocative insights into the alkylation that could not be gleaned experimentally. Most important, a number of monomer- and dimer-based alkylations of various solvation numbers are calculated to be viable. One of the more compelling themes is that lithioimine subunits bearing η^1-bound lithiums can be alkylated, whereas the corresponding η^3-bound lithioimine subunits are unreactive. However, π complexation is still mechanistically important. The ancillary subunit of the dimer—the subunit not directly involved in the alkylation— can be either η^3- or η^1-bound with accompanying mono- or disolvation. The alkylations can be either endocyclic via a medium ring (**34**) or exocyclic to an intact Li_2N_2 ring (**37**). The former shows a distinct Li−Br contact, whereas the latter does not. Monomer-based alkylations are, by comparison, relatively simple with the syn oriented disolvate, **32**, predicted to be preferred.

The mechanistic studies, especially the computational studies, address an issue that has lingered for decades. Although it is established that lithioimines alkylate syn to the *N*-alkyl moiety (eq 1),[7] the sources of the selectivity have been debated. Houk, Fraser, and co-workers proposed a high inherent preference for the lithioimine to orient the *N*-alkyl moiety syn to the carbanion.[8c,d] Glaser et al. suggested that syn alkylations may derive from aggregation effects.[8a] The calculations are in full accord with experiment by showing a dominance of syn alkylation *regardless of aggregation and solvation numbers*. The origins of the syn selectivity may be quite simple: the approach of the alkylating agent proximate to the *N*-isopropyl moiety of the syn form may be sterically less demanding than the approach proximate to the Li fragment bearing solvents (as in the monomer) or solvents and an ancillary lithioimine subunit (as in the dimer; eq 15). Consequently, the syn alkylation may be preferred simply owing to steric approach control.

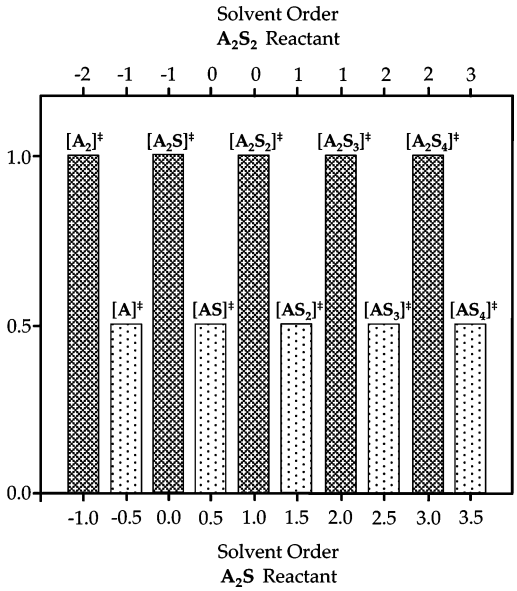

Figure 10. Plot of organolithium reaction order vs solvent order illustrating the relationship between reagent structures, reaction orders, and stoichiometries of the transition structures.

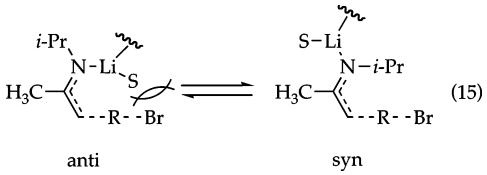

(15)

Comments on the Rate Laws. The large number of variations within the transition structures attests to the mechanistically "rich" chemistry of lithioimines, but that may not be the entire story. One of the fundamental tenets of kinetics is that the rate law provides the stoichiometry of the rate-limiting transition structure relative to the reactants.[35] When an $\mathbf{A_2S}$ dimer-based reagent is used, each dimer-based pathway has an affiliated order in solvent that is a conventional-looking integer value. By contrast, the monomer-derived pathways display seemingly odd fractional solvent orders. Although these may seem like simple algebraic artifacts, the choice of starting material can have an influence beyond simply altering the mathematical form of the rate law.

Figure 10 illustrates what is likely to be the first (and only!) plot of organolithium reaction orders versus solvent reaction orders. Even casual inspection of the plot reveals how a change in solvent concentration or even a change in solvent polarity—

(35) Espenson, J. H. *Chemical Kinetics and Reaction Mechanisms*, 2nd ed.; McGraw-Hill: New York, 1995.

an act tantamount to moving along the *x*-axis—might cause changes in mechanism with affiliated changes in the rate laws. There is a more subtle point to be made having to do with the fundamental differences between $\mathbf{A}_2\mathbf{S}_2$ and $\mathbf{A}_2\mathbf{S}$ as starting materials.

Let us first focus on the *x*-axis listed along the top edge of Figure 10, in which the orders stem from using $\mathbf{A}_2\mathbf{S}_2$ starting material as found in normal lithium amides. The solvent orders are integer values, and there exists both a monomer- and a dimer-based pathway for each value. For any fixed solvent order there is necessarily a natural tension between monomer- and dimer-based chemistry. Changes in solvent concentration or polarity can introduce new competing pathways, but the solvent-dependent changes in mechanism require integer changes in solvent order.

Now focus on the lower *x*-axis, which illustrates the relationship of solvent and organolithium orders starting from an $\mathbf{A}_2\mathbf{S}$ dimer. The solvent orders are spaced in *half*-integer units and each solvent order *uniquely* defines a monomer- or dimer-based transition structure. Changing solvent concentration causes an alternating shift between monomer- and dimer-based mechanisms in half-integer increments, increasing the likelihood of solvent-dependent changes in mechanism. From a purely algebraic perspective, the distribution of mechanisms is influenced by the choice of $\mathbf{A}_2\mathbf{S}$ versus $\mathbf{A}_2\mathbf{S}_2$ reagents.[36]

Conclusions

We are often asked to condense what we have learned about organolithium solution structure and mechanism into a set of simple rules. The problem is that there are *many* simple rules, and the chemistry of lithioimines appears to be a referendum on this diversity. Given the number of issues presented by lithioimines—the stereochemistry about the C−N bond, solvation numbers, aggregation state, stereochemistry of aggregation, hapticity—and given that these issues are present in both the reactants and transition structures, it is extraordinary that lithioimines have proven to be such useful and versatile reactive intermediates.[6] We began this paper with the casual observation that the alkylation of lithiated *N*-phenylimine **1** affords a mixture of N- and C-alkylated products. Are we ready to investigate this selectivity? The results on the C-alkylation of **3** described herein suggest the task is *still* daunting.

(36) The relationship of the rate law to the starting material was illustrated by LiTMP-mediated epoxide eliminations that proceed via $[\mathbf{A}_2\mathbf{S}]^{\ddagger}$. Differing starting materials—$\mathbf{A}_4$ in Me_2NEt versus $\mathbf{A}_2\mathbf{S}_2$ in THF—afford rate laws of profoundly different mathematical forms. See ref 4b.

Experimental Section

Reagents and Solvents. Alkyl halides were distilled and stored as stock solutions in toluene. Ethereal solvents and toluene were distilled by vacuum transfer from blue or purple solutions containing sodium benzophenone ketyl. LDA and [^{6}Li]LDA were purified using recrystallization.[9] The preparation of lithioimines **3**, [^{6}Li]**3**, and [^{6}Li,^{15}N]**3**, as well as their corresponding imines **5** and [^{15}N]**5** is described in the Supporting Information. The diphenylacetic acid used to check lithioimine solution titers was recrystallized from methanol and sublimed at 120 °C under full vacuum.[37] Air- and moisture-sensitive materials were manipulated under argon using standard glovebox, vacuum line, and syringe techniques.

NMR Spectroscopic Analyses. Samples were prepared and the ^{1}H and ^{13}C NMR spectra were recorded as described in the Supporting Information. ^{6}Li and ^{15}N NMR experiments are also archived in the Supporting Information.

Kinetics. Rate studies were carried out by monitoring the loss of alkyl halides relative to an internal decane standard as described previously.[29]

Acknowledgment. We thank the National Institutes of Health for direct support of this work as well as DuPont Pharmaceuticals, Merck Research Laboratories, Pfizer, Aventis, R. W. Johnson, Boehringer-Ingelheim, and Schering-Plough for indirect support.

Supporting Information Available: Experimental procedures, NMR spectra, rate data, tabular and graphical presentation of computational results, and X-ray crystallographic data. This material is available free of charge via the Internet at http://pubs.acs.org.

JA060363K

(37) Kofron, W. G.; Baclawski, L. M. *J. Org. Chem.* **1976**, *41*, 1879.